PAPER

CrossMark
click for updates

The utility of dimolybdenum *tetrakis*(μ-isovalerate) and *tetrakis*(μ-pivalate) in the stereochemical studies of various transparent compounds†

Magdalena Jawiczuk, Joanna E. Rode, Agata Suszczyńska, Adam Szugajew‡
and Jadwiga Frelek*

The aim of the present work was to verify the usefulness of dimolybdenum *tetrakis*(μ-pivalate) and *tetrakis*(μ-isovalerate) as auxiliary chromophores for determining the absolute configuration of optically active *vic*-diamines, *vic*-amino alcohols, α-amino and α-hydroxy acids by means of electronic circular dichroism (ECD). To this end, a series of measurements designed to check the dependence of ECD and UV-Vis spectra on time and concentration was carried out. The experimental results were supported by a separate set of detailed DFT calculations. The results obtained allowed us to determine the most probable structure of dominating chiral complexes formed *in situ* in solution for all ligands studied.

1. Introduction

The progress of techniques in determining absolute configuration (AC) was driven by increased attention to chiral molecules. The connection between the stereochemistry of such compounds and their physical, chemical and biological properties has led to further exploration of methods for determining the three-dimensional structure. Chiroptical spectroscopy has been successfully applied for solving stereochemical problems, and has proven to be a sensitive, fast and useful technique. Nowadays, it is generally accepted that use of at least two different chiroptical techniques (ECD, VCD, VROA) in tandem with quantum-chemical calculations is the safest way to unambiguously assign the AC of the compounds tested.[1] However, there will always be some compounds whose stereochemistry cannot be unequivocally attributed despite the use of several different spectroscopic methods. Therefore, it is essential to explore new chiroptical methods in order to achieve a greater number of techniques,[2] allowing the use of several of them to more reliably determine the AC.[1]

The assignment of AC of molecules transparent in the UV-Vis range by electronic circular dichroism (ECD) requires their transformation into chromophoric derivatives. For such compounds the exciton chirality method (ECCD) has found broad applicability, due to the very characteristic shape of the CD bands, large Cotton effects (CEs) and its non-empirical character.[3] However, some conformationally flexible molecules and acyclic compounds may cause difficulties in case of this method, or the rules established do not have general applicability.[4–6] On the contrary, the dimolybdenum methodology avoids this problem, since in the chiral Mo_2-complexes formed *in situ* the conformational mobility of ligands is restricted due to steric hindrance from the remaining carboxylate groups of the stock complex.[7] This means that mixing the chiral ligand with an achiral auxiliary chromophore, in this case one of the dimolybdenum complexes, results in conformationally defined derivatives. Thus, as an additional benefit, this *in situ* method allows the determination of the AC of an examined compound based on the ECD spectra alone.[8]

Previous studies have shown that dimolybdenum *tetrakis*-(μ-acetate) (**Mo1**) can be used as the auxiliary chromophore, as it creates optically active complexes with a wide group of transparent compounds (Fig. 1).[9,10] The drawback, however, of using **Mo1** is that it has a narrow group of solvents (DMSO, pyridine and acetic acid) in which it can be used, limiting the ability to further study the chiral structures of the analysed molecules. This limitation caused us to search for a viable alternative for dimolybdenum *tetrakis*(μ-acetate) (**Mo1**). We examined the usefulness of various dimolybdenum tetracarboxylates in identifying the AC of *vic*-diols, and compared them to the results with **Mo1**.[11]

Based on preliminary results,[11] dimolybdenum *tetrakis*-(μ-pivalate) (**Mo2**) and dimolybdenum *tetrakis*(μ-isovalerate) (**Mo3**) were selected from a variety of dimolybdenum carboxylates as the most promising (Fig. 1). They are well soluble in most common solvents used in spectroscopy as, *e.g.*, hexane, acetonitrile, chloroform, and ethanol. The results for both these

Institute of Organic Chemistry, Polish Academy of Sciences, Kasprzaka 44/52, 01-224 Warsaw, Poland. E-mail: jadwiga.frelek@icho.edu.pl; Web: http://ww2.icho.edu.pl/Frelek_group/index.html; Tel: +48-22-343-22-15

‡ Present address: Student of Materials Engineering Faculty of the Warsaw University of Technology, Wołoska 141, 02-507 Warsaw, Poland.
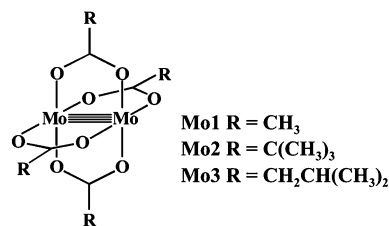
Fig. 1 Structure of investigated dimolybdenum tetracarboxylates.

complexes with *vic*-diols were similar to those for **Mo1**. Considering the intensity and the sign sequence of CEs these auxiliary chromophores are subject to the same helicity rule proposed previously for dimolybdenum *tetrakis*(μ-acetate).[11] This rule correlates the positive sign of CE around the 300 nm in the ECD spectra with a positive sign of the OH–C–C–OH torsion angle of the diol unit.[7,12–15] In addition, through experimental measurements and computational tools, the probable structure of the dominant chiral complex existing in the solution was shown to be chelated rather than bridging.[11]

Since the two complexes, *i.e.* **Mo2** and **Mo3**, were successful with the *vic*-diols we began to wonder – could they be also applied in dichroic studies for other important transparent ligands such as 1,2-diamines, 1,2-amino alcohols, α- and β-hydroxy acids or α-amino acids? These classes of ligands are of particular importance due to their interesting properties as well as their role in pharmacy,[16,17] as building blocks in synthesis,[18] in the cosmetic industry[19] or by the production of polymers.[20,21] Moreover, compounds such as α-amino acids, α- and β-hydroxy acids play an important role in the functioning of the human body, for example β-hydroxy acids serve as an energy source when blood sugar is low.[22]

In the present study both dimolybdenum *tetrakis*(μ-pivalate) and dimolybdenum *tetrakis*(μ-isovalerate) complexes were used in the analysis of the above mentioned groups of compounds and confronted with **Mo1**, as a test of their suitability. Model compounds of known AC will be examined to confirm correlation between structure and CEs in ECD spectra, subsequently allowing the application of these rules to compounds of unknown AC.

Furthermore, ECD calculations were conducted and compared with the experimental results in order to establish the structure of the dominating chiral complex created in the solution.

In the context of the above, the main objective of this work can be defined as a test of the suitability of the two dimolybdenum tetracarboxylates **Mo2** and **Mo3** as auxiliary chromophores in dichroic assignment of AC for a variety of biologically important compounds, non-absorbing in the UV-Vis spectral range. We intend to achieve this goal by examining the kinetic stability of the chiral complexes formed in solution. In addition, we will test the dependence of the shape of CD curves on the concentration ratio of ligand to stock complex. A notable result of the study is establishing the extent of applicability and potential restrictions in the use of complexes in question as auxiliary chromophores in dichroic studies.

2. Results and discussion

We began our inquiry by measuring the ECD spectra for each of the studied ligands under different measurement conditions in order to establish the best one. The conditions varied in terms of ligand-to-metal complex molar ratio, solvent and time. Based on our previous experience with *vic*-diols we noticed that the ratio of ligand to metal between 1.5 and 3 to 1 gave the best results, and so we decided to take advantage of this range of concentrations in our current work.[11] Since the solvent can cause significant differences in the spectra, the experimental measurements were performed in chloroform and acetonitrile. This choice is also in accord with our previous experience with solvents for dimolybdenum complexes.[11] Samples were measured after dissolving of components, then 1, 3 and 24 hours after, to examine the stability of the chiral complexes formed *in situ* in the solution. After initial optimization of measurement conditions and selection of the best solvent, the study of generality, sensitivity, and reliability of complexes **Mo2** and **Mo3** as auxiliary chromophores in ECD measurements of their adducts with α-amino- and α-hydroxy acids, 1,2-amino alcohols and 1,2-diamines were conducted. The results of our considerations will be presented for each type of ligands individually.
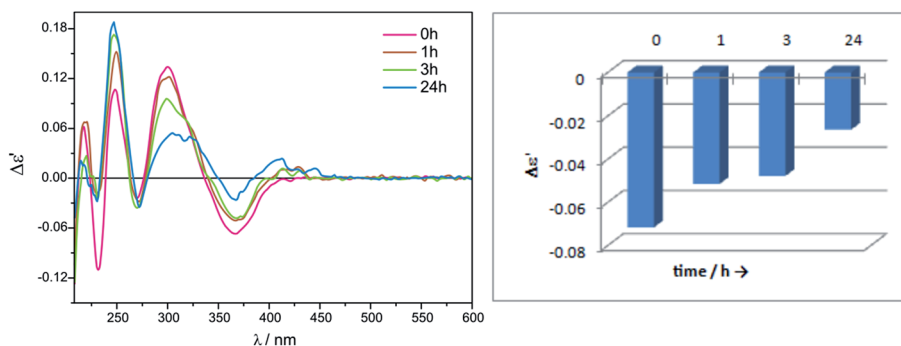

Fig. 2 Time-dependent ECD spectra of *in situ* formed Mo₂-complexes of ʟ-valine (**1**) with **Mo3** recorded in acetonitrile/water 4 : 1 ratio (left); Graphical presentation of time dependence of the ECD spectra of the ʟ-valine (**1**) complex with Mo₂-core at λ = 366.5 nm (right). The term Δε′ is explained in the Experimental section.

Table 1 UV-Vis and ECD data of *in situ* formed Mo$_2$-complexes of compounds **1–3** recorded in a mixture of acetonitrile-water 4 : 1 ratio immediately after dissolving[a]

Comp.	UV ε (λ_{max})	ECD $\Delta\varepsilon'$ (λ_{max})			
	Band A	Band I	Band II	Band III	Band IV
Mo2					
1	4440 (293.5)	+0.06 (248.5)	−0.01 (272.5)	+0.04 (299.0)	−0.03 (367.0)
2	5730 (296.0)	—	+0.05 (264.5)	−0.06 (300.0)	+0.04 (372.0)
3	4530 (298.5)	—	—	−0.19 (298.0)	+0.01 (369.0)
Mo3					
1	4540 (293.5)	+0.11 (248.5)	−0.02 (270.0)	+0.13 (300.5)	−0.07 (366.5)
2	4850 (293.0)	−0.01 (248.5)	+0.08 (268.5)	−0.02 (308.0)	+0.05 (362.5)
3	4590 (292.0)	—	—	−0.19 (293.0)	+0.06 (382.5)

[a] Values are given as $\Delta\varepsilon'$ (dm^3 mol^{-1} cm^{-1}) and λ_{max} (nm).
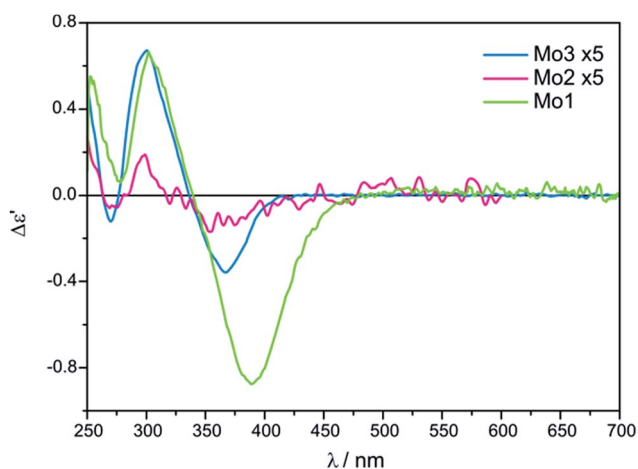

Fig. 3 Comparison of ECD spectra of *in situ* formed chiral complexes of **Mo2** and **Mo3** with L-valine (**1**) recorded in CH$_3$CN/H$_2$O (4 : 1) *versus* **Mo1** with **1** recorded in DMSO. The term $\Delta\varepsilon'$ is explained in the Experimental section.

I.   α-Amino acids

The ECD measurements of α-amino acids chosen as models for present studies (Chart 1) were conducted in a mixture of acetonitrile and water at a ratio 4 to 1 to overcome the low solubility of the substrates without the addition of water. The other solvent, *i.e.* chloroform, was completely excluded because of the total insolubility of the ligands. As a model compound for study of concentration dependence and time stability of the complexes formed *in situ* in solution L-valine (**1**) was chosen.

Because the general shape of ECD curves is unchanged for both concentrations of ligand *versus* stock complex, *i.e.* 1.5 : 1 and 3 : 1, for either **Mo2** or for **Mo3**, we decided to carry out the
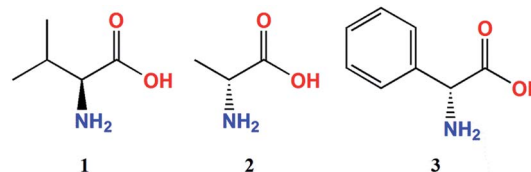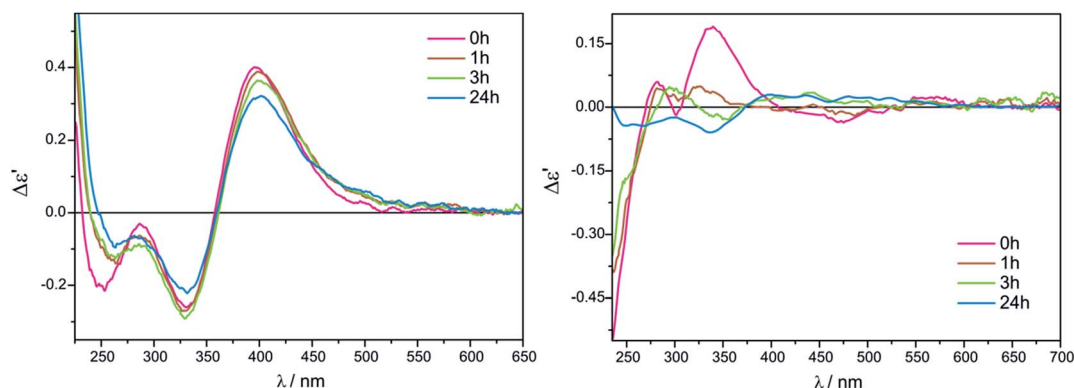

Chart 1   Investigated α-amino acid ligands.

Fig. 4 Time-dependent ECD measurements of *in situ* formed Mo$_2$-complexes of L-lactic acid (**5**) with **Mo3** in CH$_3$CN (left) and in CHCl$_3$ (right) in 1.5 : 1 ligand-to-metal molar ratio. The term $\Delta\varepsilon'$ is explained in the Experimental section.

measurements with lower concentration for economic reasons. The chiral complexes formed *in situ* were stable within the examined time period, or a slight decrease in the intensity of bands in the diagnostic spectrum range ~300−450 nm was observed, as presented in Fig. 2 and S1 in ESI†. Summarising, we conducted the experiments with the remaining α-amino acid ligands under optimised conditions, namely in 1.5 : 1 ligand-to-stock complex molar ratio, and after the dissolution of constituents in a mixture of acetonitrile with water 4 : 1.

In the absorption spectra of stock complexes **Mo2** and **Mo3** three absorption bands are present. The first one, of weak intensity and occurring at *ca.* 440 nm (band B), is assigned to the δ → δ* transition whereas the more intense absorption band appearing at around 300 nm (band A) is attributed to the π → π* electronic transition.[23] The third absorption band, present as a shoulder at longer wavelengths of band A and assigned to the δ → π* transition, occurs at ~325 nm.[23] However, in the spectra of adducts resulting from coordination of the various amino acids ligands to **Mo2** and **Mo3** practically only one absorption band is visible, namely band A (Table 1). On the other hand, in the range of 240–420 nm examined α-amino acids (Chart 1) give from two to four CEs with **Mo2** and **Mo3** (Table 1). For determining the absolute configuration, the most suitable bands are those near 300 and 370 nm because they are present in the spectra of all α-amino acids tested (Fig. 3 and Table 1).

The conclusive CEs for L-α-amino acids at around 370 and 300 nm are negative and positive respectively. Accordingly, the inverse signs sequence in the same spectral range applies to their D counterparts. Thus, the results obtained for **Mo2** and **Mo3** confirm that they are subject to the same correlating rule as **Mo1** (Fig. 3).[10]

Despite the bands of dimolybdenum *tetrakis*(μ-pivalate) **Mo2** and *tetrakis*(μ-isovalerate) **Mo3** with all tested α-amino acids exhibiting the same CE sign sequence, they are generally less intensive than those of dimolybdenum tetraacetate **Mo1**. Moreover, due to the poorly developed bands and their very low intensity, **Mo2** does not constitute a viable alternative auxiliary chromophore for this group of ligands (Fig. 3). On the contrary, **Mo3** can be considered as an alternative to **Mo1** because the diagnostic bands are well developed although their lower intensity.

II. α-Hydroxy acids

The measurement conditions for the next group of ligands, *i.e.* α-hydroxy acids presented on Chart 2, were maintained as for α-amino acids, with the exception that both acetonitrile and chloroform were used as solvents.

The ECD bands at 330 nm and 400 nm for **Mo2** (Fig. S2 in ESI†) and **Mo3** in acetonitrile are fully resolved and clearly visible. Moreover, in this solvent, the intensity of ECD bands changes insignificantly with time for both examined auxiliary
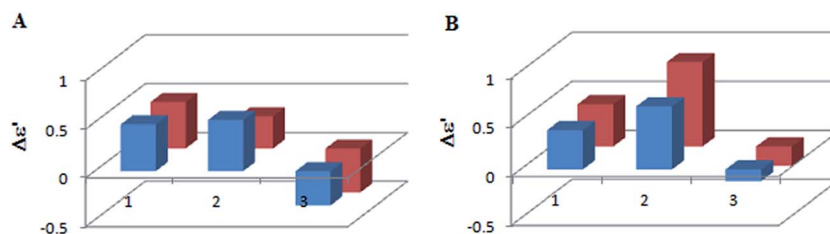

Fig. 5 Concentration dependency for L-lactic acid (row 1), L-mandelic acid (row 2) and *R*-butyric acid (row 3) with **Mo2** (A) and **Mo3** (B) complex for ECD band IV, *i.e.* at ~360 nm; 1.5 : 1 ligand-to-complex molar ratio (blue), 3 : 1 ratio (red) recorded immediately after mixing of components. The term Δε′ is explained in the Experimental section.

Table 2 UV-Vis and ECD data of *in situ* formed Mo₂-complexes of compounds 4−6 recorded in acetonitrile immediately after dissolving[a]

Comp.	UV ε (λ_max)	ECD Δε (λ_max)					
	Band A	Band I	Band II	Band III	Band IV	Band V	Band VI
Mo2							
4	4470 (304.0)	+ 0.98 (272.5)[sh]	—	(335.5)[a]	+0.52 (390.0)	−0.06 (517.0)	−0.13 (632.0)
***ent*-4**	4520 (306.0)	−1.29 (270.0)[sh]	—	+0.03 (336.0)	−0.53 (394.0)	+ 0.05 (516.5)	+0.05 (633.0)[b]
5	4590 (306.5)	−0.28 (253.0)	—	−0.24 (320.0)	+0.48 (392.5)	−0.01 (528.5)	—
6	5410 (293.0)	+0.73 (233.0)	−0.01 (292.0)	+0.10 (323.0)	−0.35 (394.0)	—	—
Mo3							
4	4660 (303.0)	+1.39 (271.5)[sh]	—	−0.07 (335.0)	+0.64 (390.0)	−0.02 (524.0)	−0.07 (630.5)[b]
***ent*-4**	3750 (304.0)	−1.00 (271.0)[sh]	—	+0.10 (333.0)	−0.62 (389.0)	+0.05 (524.0)	+0.06 (631.0)
5	4740 (303.5)	−0.22 (253.5)	—	−0.26 (330.5)	+0.40 (395.5)	—	—
6	1810 (298.0)	+0.43.5 (243.5)	−0.01 (299.0)	+0.06 (335.0)	−0.12 (400.5)	—	—

[a] Values are given as Δε′ (dm³ mol⁻¹ cm⁻¹) and λ_max (nm); [sh] inflection point, [a] local maximum. [b] Developed after 24 h.
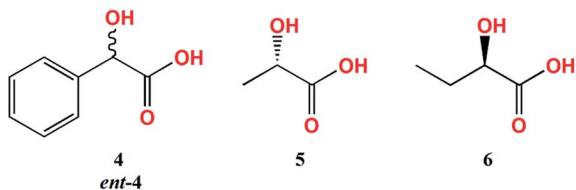
Chart 2 Investigated α-hydroxy acid ligands; **4** = L-mandelic acid, **ent-4** = D-mandelic acid.

chromophores, which can be seen in the case of Mo$_2$-complexes of L-lactic acid (**5**) in Fig. 4 (left).

On the other hand, in chloroform as a solvent, ECD bands at around 410 nm are very poorly developed and overlap in the diagnostic spectral range. In addition, in chloroform the CD pattern and the intensity of bands changed quite significantly during the investigated 24 hours (Fig. 4, right).

To establish whether the shape of CD curves depends on the concentration ratio, the CD spectra of L-lactic acid (**5**),
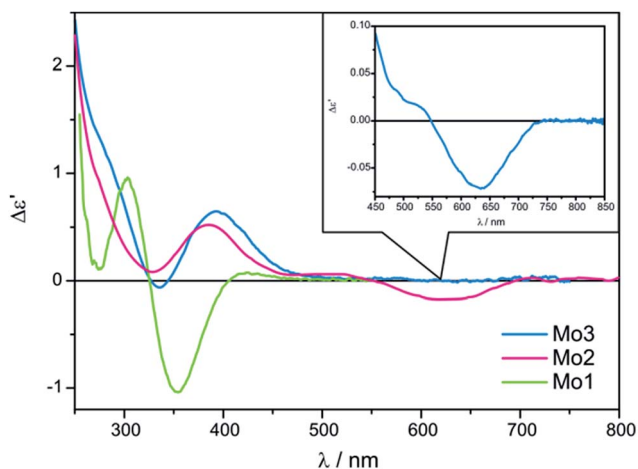
L-mandelic acid (**4**) and *R*-butyric acid (**6**) with the Mo$_2$-core in 1.5 : 1 and 3 : 1 ligand-to-metal ratios were recorded. The results show that increasing the concentration of the ligand does not change the ECD curve or cause a significant change in the intensity of the corresponding CEs (Fig. 5).

On the basis of the results presented above it was concluded that the 1.5 : 1 molar ratio of the constituents is convenient for chiroptical study of α-hydroxy acids. Moreover, ECD measurements can be conducted immediately after chiral complex formation. In order to avoid misleading interpretation caused by changing ECD bands in chloroform for this class of compounds it is recommended to use acetonitrile as a solvent of choice.

In most cases, α-hydroxy acids yield up to four CEs in the range of 230–650 nm with **Mo3**, and up to five with **Mo2**. The most intense and therefore the most suitable bands to determine the AC at the α carbon of the α-hydroxy acids appear in the spectral range between 400 and 330 nm, see Fig. 4 (left) and Table 2.

For L-mandelic acid (**4**), a broad CE at ∼630 nm can be observed in the ECD spectrum (Fig. 6). This band appears right after dissolution for the complex **Mo2**, while for **Mo3** it develops fully after 24 hours. Inversely, the D enantiomer (**ent-4**) develops this ECD band immediately after reconstitution with **Mo3** and overnight for **Mo2** (Table 2).

The ECD spectra of examined ligands (Chart 2) with either dimolybdenum tetracarboxylate **Mo2** as well as **Mo3** are shifted towards higher energy spectral range compared to spectra recorded with the use of dimolybdenum tetraacetate **Mo1** (Fig. 6). From the viewpoint of the relationship between structure and signs of CEs such a shift towards lower energy is undoubtedly an advantage.

Based on the above mentioned results the correlation between the signs of particular CEs and configuration of α-hydroxy acids can be formulated as follows: with **Mo2** or **Mo3** as auxiliary chromophores, all L-α-hydroxy acids give a positive CE of around 400 nm and a negative one near 330 nm. For D-α-hydroxy acids an opposite sign pattern is observed (Table 2).

In conclusion, both complexes **Mo2** and **Mo3** display the conformity of signs of individual absorption bands coherent

Fig. 6 Comparison of ECD spectra of *in situ* formed chiral complexes of **Mo2**–**Mo3** with L-mandelic acid (**4**) recorded in CH$_3$CN *versus* **Mo1** with **4** recorded in DMSO. The term $\Delta\varepsilon'$ is explained in the Experimental section.
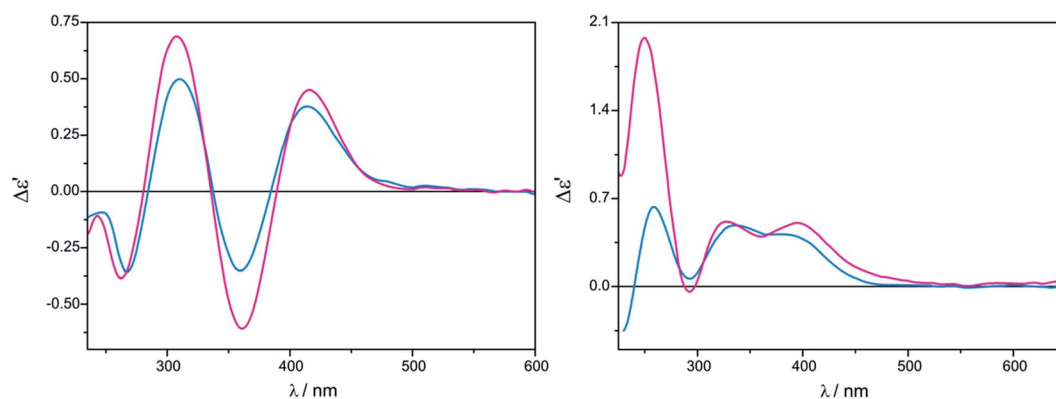

Fig. 7 Concentration dependency for D-alaninol (**7**) with **Mo2** complex recorded in CHCl$_3$ (left) and in CH$_3$CN (right); 1.5 : 1 ligand-to-complex molar ratio (blue), 3 : 1 ratio (purple). The term $\Delta\varepsilon'$ is explained in the Experimental section.

with the operating hexadectant rule[10,24] and can be applied as effective replacements of **Mo1** (Fig. 6).

III.   1,2-Amino alcohols

Another group of compounds, which were a subject of our investigation are *vic*-amino alcohols whose selected representatives are depicted in Chart 3.

In the case of *tetrakis*(μ-pivalate) **Mo2** the most intense and fully resolved bands are observed in chloroform for 1.5 : 1 ligand-to-metal molar ratio (Fig. 7, left). Shifting concentration to 3 : 1 does not cause changes in the shape of the ECD bands, but induces a small upswing of their intensities (Fig. 7). In acetonitrile the intensity of ECD bands in 300–500 nm energy
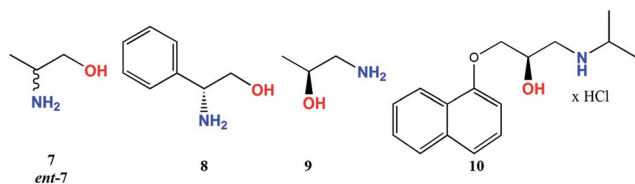
range changes insignificantly with increased ligand concentration (Fig. 7).

The intensity of short-wavelength ECD bands changed slightly over time in acetonitrile. More substantial changes, and some decrease of band intensities was observed during the 24 hours in chloroform, as can be seen in Fig. 8.

On the contrary, in the presence of **Mo3**, well developed CEs occur in acetonitrile (Fig. 9, right), while in chloroform ECD bands are less intense and not entirely resolved (Fig. 9, left). In addition, a similar time and concentration-dependence as for **Mo2** can be observed in this case (Fig. S3 in ESI†).

In order to avoid misleading interpretation of results, it is recommended that ECD spectra be measured after dissolution with 1.5 : 1 ligand-to-metal molar ratio in chloroform for **Mo2** and acetonitrile for **Mo3** as a solvent of choice.

(*R*)-Propranolol (**10**) was measured only in CHCl₃ in the form of hydrochlorides and in the form of free amine (obtained *in situ* after addition of a drop of aqueous base to the solution). Similar shape with different intensity of the ECD curves was received in both forms of amine for **Mo2** and **Mo3** (Fig. 10).

ECD band intensity of hydrochloride increases with time, whereas the free amine shows a decrease in 24 hours (ESI Fig. S4–S5†). In the spectra of compound **10**, bands around 270−300 nm cannot be seen as they are obscured by own
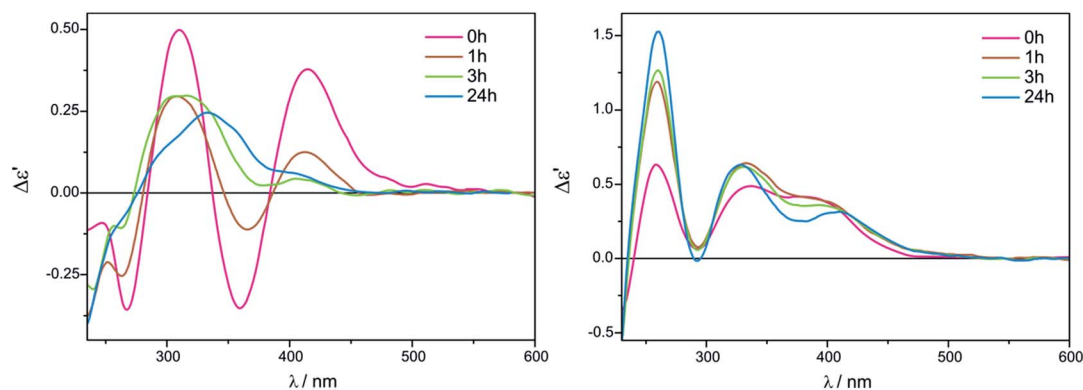

Chart 3   Investigated 1,2-amino alcohol ligands; **7** = D-alaninol, *ent*-**7** = L-alaninol.

Fig. 8   Time-dependency for compound **7** with **Mo2** recorded in CHCl₃ (left) and in CH₃CN (right) for 1.5 : 1 ligand-to-complex molar ratio. The term $\Delta\varepsilon'$ is explained in the Experimental section.
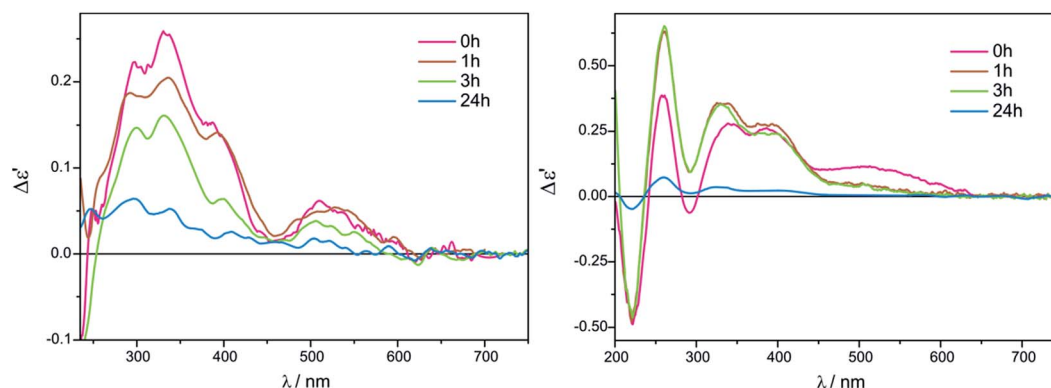

Fig. 9   Time dependency for compound **7** with **Mo3** recorded in CHCl₃ (left) and in CH₃CN (right) for 1.5 : 1 ligand-to-complex molar ratio. The term $\Delta\varepsilon'$ is explained in the Experimental section.
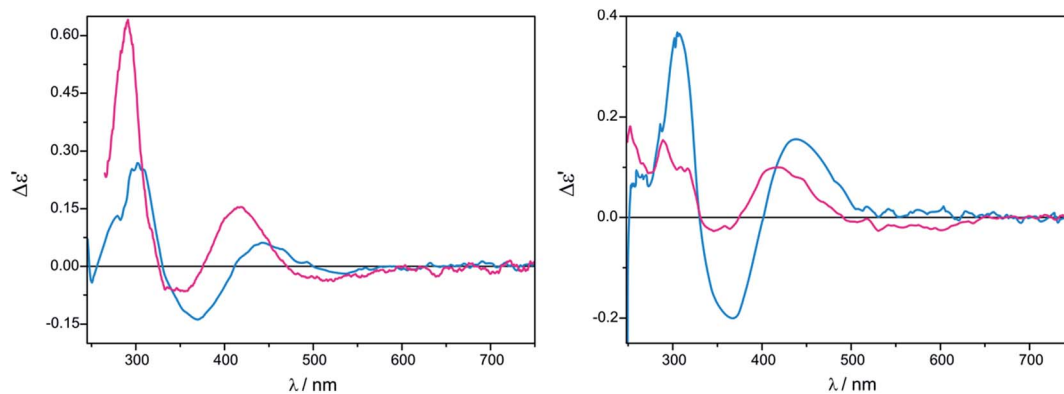
Fig. 10   ECD spectra of *in situ* formed Mo$_2$-complexes of **Mo2** (left) and **Mo3** (right) with (*R*)-propranolol (**10**) recorded in CHCl$_3$ without (purple line) and with (blue line) a trace of alkali. The term $\Delta\varepsilon'$ is explained in the Experimental section.

Table 3   UV-Vis and ECD data of *in situ* formed Mo$_2$-complexes of compounds **7–10** recorded after dissolving (**Mo2** in CHCl$_3$, **Mo3** in CH$_3$CN)[a]

Comp.	UV ε (λ_{max}) Band A	ECD $\Delta\varepsilon$ (λ_{max}) Band I	Band II	Band III	Band IV	Band VI
Mo2						
7	6660 (297.0)	−0.30 (267.5)	—	+0.55 (310.0)	−0.30 (359.5)	+0.43 (415.0)
ent-7*	5800 (302.6)	+0.20 (266.5)	—	−0.54 (309.0)	+0.25 (360.0)	−0.38 (414.5)
8	7540 (299.0)	−0.90 (269.5)	—	(300.0)[b,c]	−0.41 (361.5)	+0.29 (418.5)
9	5800 (302.0)	+0.14 (264.5)	−0.15 (295.5)	(324.0)[b]	−0.09 (361.0)	—
10[a]	4560 (331.5)[d]	—	e	e	−0.07 (354.0)	+0.15 (418.0)
Mo3						
7	4490 (308.0)	+0.38 (261.0)	—	−0.06 (292.0)	+0.28 (339.0)	+0.26 (386.0)
ent-7*	4290 (308.0)	−0.38 (258.0)	—	+0.01 (291.5)	−0.28 (338.0)	−0.25 (384.0)
8	4900 (302.5)	+0.43 (258.0)	—	(291.0)[f]	+0.33 (337.0)	+0.33 (397.0)
9	4510 (306.5)	−0.07 (260.5)	−0.09 (285.0)	+ 0.01 (319.5)	−0.18 (374.5)	+0.06 (455.5)
10[a]	3170 (339.0)[g]	—	e	e	−0.03 (346.0)	+0.10 (418.5)

[a] Values are given as $\Delta\varepsilon'$ (dm^3 mol^{-1} cm^{-1}) and λ_{max} (nm); [a] without trace of alkali, [b] negative maximum, [c] additional inflection point at *ca.* 315.0 nm, [d] additional UV-Vis band at 479.5, [e] own electronic absorption, [f] positive minimum, [g] additional UV-Vis band at 472.5 nm, * due to turbidity of the solution results should be treated as qualitative.
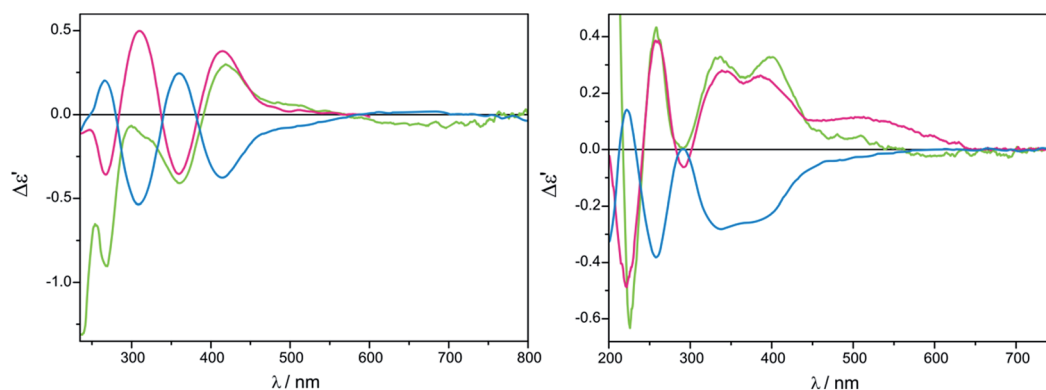

Fig. 11   Comparison of ECD spectra of *in situ* formed chiral complexes of D-alaninol (**7**, pink line), L-alaninol (***ent*-7**, blue line) and D-α-phenylglycinol (**8**, green line) with **Mo2** (left) recorded in CHCl$_3$ and with **Mo3** (right) recorded in CH$_3$CN. The term $\Delta\varepsilon'$ is explained in the Experimental section.
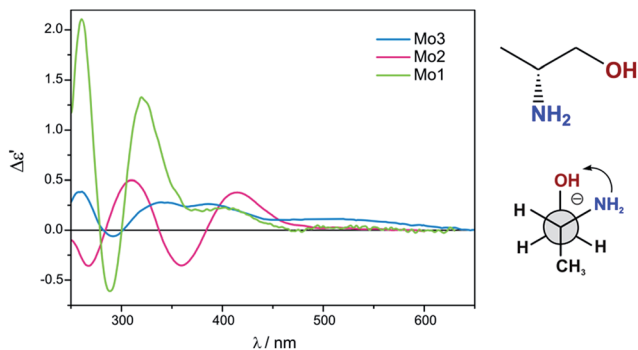
Fig. 12 Comparison of ECD spectra of *in situ* formed chiral complexes of D-alaninol (**7**) with **Mo2** (in CHCl₃) and **Mo3** (in CH₃CN) *versus* **Mo1** with **7** (in DMSO). The term $\Delta\varepsilon'$ is explained in the Experimental section.

electronic absorptions of **10** in the specified spectral range (ESI Fig. S6†). Results collected in Table 3 demonstrate that the examined 1,2-amino alcohols exhibit up to six CEs in the 250–600 nm spectra range. (Fig. 11). The most suitable for structure-chiroptical properties correlation are the ECD bands occurring in the 300–500 nm spectral range since, being adequately intensive, they occur in the spectra of all model compounds tested.

For **Mo3** with *vic*-amino alcohols, the empirical correlation between signs of particular CEs and the torsional angle N–C–C–O can be formulated as follows: a positive (negative) torsional angle of amino alcohol subunits correlates with a negative (positive) sign of the CE around 300 nm and a positive (negative) of around 340 nm (Fig. 12). Dimolybdenum *tetrakis*(μ-pivalate) (**Mo2**) with *vic*-amino alcohols is the subject to the same regularity as **Mo3**.

The proposed helicity rule is based on the ECD spectra of acyclic *vic*-amino alcohols of both ephedrine and adrenaline types, complexed with Mo₂-core, and it is consistent with the rule proposed previously for **Mo1**.[24] Thus, we are entitled to conclude that the two dimolybdenum tetracarboxylates **Mo2** and **Mo3** are an efficient alternative to **Mo1**.

IV. 1,2-Diamines

The last group of examined ligands are *vic*-diamines presented in Chart 4. Beside dimolybdenum *tetrakis*(μ-pivalate) **Mo2** and *tetrakis*(μ-isovalerate) **Mo3** also dimolybdenum *tetrakis*(μ-acetate) **Mo1** was investigated with this class of compounds as it has not been examined previously. Due to the limited solubility of **Mo1** measurements were conducted in DMSO.

(2*S*)-3-phenylpropane-1,2-diamine (**13**) was chosen as a model diamine for preliminary studies on the solubility, stability and the influence of the chiral ligand concentration on the resulting ECD spectra. As before, both acetonitrile and chloroform solvents for **Mo2** and **Mo3** were tested. For all three complexes **Mo1**–**Mo3** two chiral ligand-to-metal ratios, namely 1.5 : 1 and 3 : 1 were checked. Time stability of the complexes formed *in situ* was examined immediately after mixing of components and after 1, 3 and 24 hours. The result of this research was establishing the optimum measurement conditions for this class of compounds.

As a solvent of choice in this case we recommend to use chloroform as it causes the full development of at least two ECD bands for both complexes **Mo2** and **Mo3**, whereas in acetonitrile in the most suitable range for establishing a correlation, *i.e.* above 300 nm, only one well resolved CE within a reasonable time is yielded (Fig. 13).
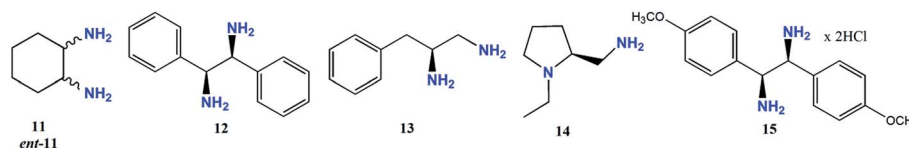

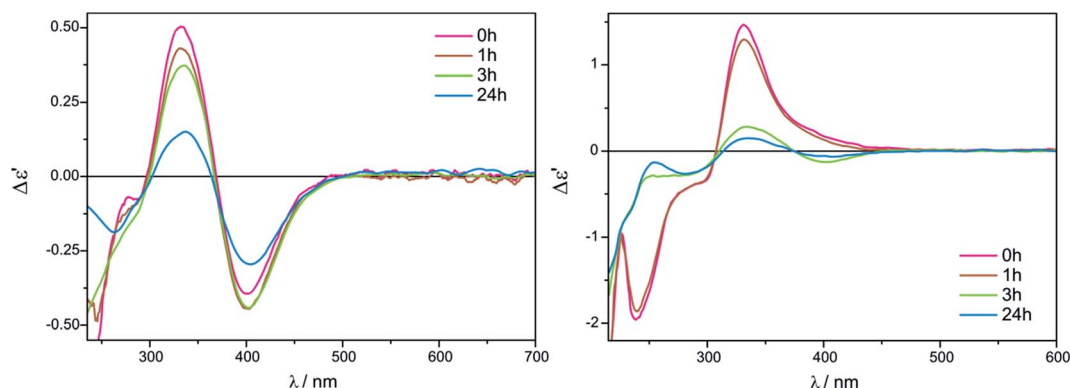**Chart 4** Investigated *vic*-diamine ligands; **11** = (1*S*,2*S*)-DACH, ***ent*-11** = (1*R*,2*R*)-DACH.

Fig. 13 Time and solvent-dependence ECD measurements of *in situ* formed Mo₂-complexes of compound **13** with **Mo3** in CH₃CN (right) and in CHCl₃ (left) in 1.5 : 1 ligand-to-metal molar ratio. The term $\Delta\varepsilon'$ is explained in the Experimental section.
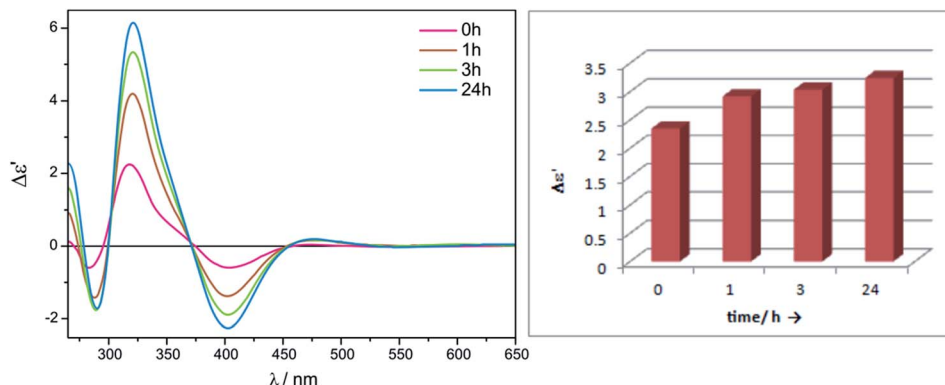
Fig. 14 The time-dependent ECD spectra of *in situ* formed complex of compound **12** with **Mo2** (left) and bar charts showing time-dependency for chiral complex formed with **Mo3** (right) at $\lambda_{max} = 323$ nm recorded in CHCl$_3$ for 1.5 : 1 ligand-to-complex molar ratio. The term $\Delta\varepsilon'$ is explained in the Experimental section.

Table 4 UV-Vis and ECD data of *in situ* formed Mo$_2$-complexes of diamines **11–15** recorded in CHCl$_3$ for **Mo2–Mo3** after compounds dissolving, and in DMSO for **Mo1** after 1 h in the range 280–500 nm[a]

Comp.	UV ε (λ_{max})		ECD $\Delta\varepsilon$ (λ_{max})				
	Band A	Band B	Band I	Band II	Band III	Band IV	Band V
Mo1							
11	3500 (295.0)	412 (385.0)	−0.49 (285.5)[sh]	—	+0.64 (331.5)	−0.15 (396.0)	+0.04 (452.0)
ent-11	2190 (295.0)	—	+0.53 (283.0)	—	−0.39 (324.0)	+0.15 (394.5)	+0.02 (450.0)[sh]
12	4600 (303.0)	177 (434.0)	+0.57 (279.5)[sh]	—	+4.74 (322.0)	−0.63 (398.5)	+0.32 (494.0)
13	5500 (298.0)[a]	125 (438.0)	—	—	+0.08 (351.5)	−0.12 (402.0)	−
14	5080 (303.0)	251 (439.0)	+0.05 (297.0)	—	−0.06 (354.0)	—	+0.01 (461.5)
15	5420 (299.0)	383 (437.0)	+1.74 (274.0)	+1.07 (308.5)	—	−1.04 (400.0)	−
Mo2							
11	4590 (296.0)	820 (456.5)	−0.78 (281.0)	—	+0.28 (342.0)	−0.27 (402.5)	−
ent-11	4700 (297.0)	910 (457.0)	+0.68 (279.0)	—	−0.30 (342.0)	+0.30 (403.5)	−
12	5260 (296.5)	795 (449.0)	−0.59 (283.0)	+2.25 (318.0)	+0.72 (348.0)[sh]	−0.59 (404.5)	−
13	4390 (299.0)	730 (469.0)	−0.12 (290.5)	—	+0.23 (345.5)	−0.19 (409.5)	−
14	4670 (297.0)	663 (466.0)	(286.5)[b]	−0.24 (307.0)	—	+0.12 (391.0)	+ 0.11 (439.0)
15	4340 (299.5)	—	+0.99 (293.0)[c]	−0.24 (333.0)	(343.5)[b]	−0.57 (387.5)	−
Mo3							
11	4270 (302.0)	819 (472.5)	−0.67 (260.0)	−0.18 (300.0)[sh]	+0.22 (340.5)	−0.40 (401.5)	−
ent-11	4530 (300.0)	781 (450.0)	+ 0.77 (257.0)	+0.24 (300.0)[sh]	−0.26 (341.0)	+0.40 (403.0)	−
12	5280 (300.0)	700 (438.0)	−0.51 (291.0)	—	+2.35 (323.0)	−1.43 (400.0)	+0.01 (485.0)
13	4590 (299.0)	530 (468.0)	(288.5)[b]	—	+ 0.50 (332.0)	−0.39 (398.5)	−
14	4220 (304.5)	—	−	−0.28 (304.5)	—	+0.18 (386.5)	+0.09 (463.0)[sh]
15	6460 (295.0)	77 (429.0)	+0.95 (291.5)[d]	—	+0.11 (335.0)[sh]	−0.69 (386.5)	−

[a] Values are given as $\Delta\varepsilon'$ (dm^3 mol^{-1} cm^{-1}) and λ_{max} (nm); [sh] inflection point, [a] additional inflection point at 321.5 nm, [b] negative maximum, [c] additional negative CD at 284.0 nm, [d] additional positive minimum at 285.0 nm.

The shape of ECD curves vary within 24 h; for compounds **11**, **11-ent**, **13** and **14** intensity of the CEs decrease with time, while for **12** they grow for 1.5 : 1 ligand-to-metal molar ratio (Fig. 14).

As observed, *vic*-diamines in the salt form cannot be investigated by *in situ* methodology. However, in the form of free amine (obtained *in situ* after addition of a drop of aqueous base to the salt solution) ECD study can be performed successfully (Table 4).

The stability of the complexes formed *in situ* with **Mo1** was tested on the example of (1R,2R)-diaminocyclohexane (**ent-11**).

As can be seen in Fig. 15 the biggest difference in the intensity of ECD band occurs within the first hour of reconstitution and is not so substantial later on. That is why we decided to measure *vic*-diamines with dimolybdenum *tetrakis*(μ-acetate) **Mo1** 1 h after dissolution of the components.

The (S)-(−)-2-aminomethyl-1-ethylpyrrolidine (**14**), compared to other tested diamines, gives the weakest CEs with all three dimolybdenum complexes (Table 4). This may result from poor complexation of the ligand(s), as the ethyl substituent limits access to the nitrogen atom. Its ECD spectra recorded with **Mo2**
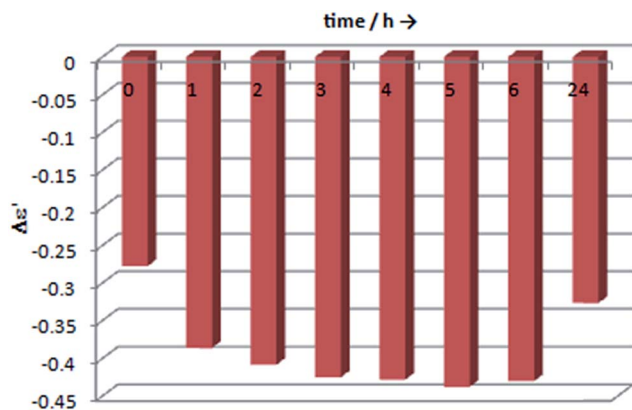
Fig. 15 Graphical presentation of the time-dependent ECD spectra of *in situ* formed complex of (1*R*,2*R*)-DACH (*ent*-11) with Mo1 at $\lambda_{max} = 325$ nm for 1.5 : 1 ligand-to-complex molar ratio. The term $\Delta\varepsilon'$ is explained in the Experimental section.
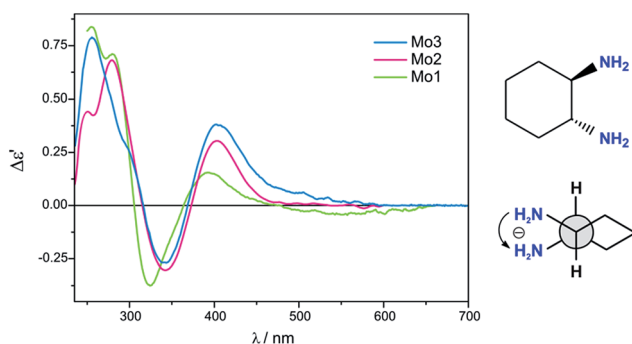

Fig. 16 Comparison of ECD spectra of *in situ* formed chiral complexes of (1*R*,2*R*)-DACH (*ent*-11) with Mo2–Mo3 recorded in CHCl₃ and with Mo1 recorded in DMSO. The term $\Delta\varepsilon'$ is explained in the Experimental section.

and Mo3 were shifted towards higher energy spectral range compared to spectra of other diamines (Table 4).

Also, we examined our alternative carboxylates Mo2 and Mo3 with optically active salts of *vic*-diamine (15). It forms Mo₂-complexes very slowly and with low efficiency, however adding a trace of alkali results in rapid development of several intense CEs (Table 4 and Fig. S7 in ESI†).

The most suitable band for the correlation between structure and sign of CEs in the ECD spectra of Mo₂-complexes with *vic*-diamines, occurs at around 340 nm. A positive torsion angle of the diamine subunit N–C–C–N correlates with a positive CE at around 330 and a negative one at *ca.* 400 nm. For a negative torsion angle of the diamine subunit an inverse relationship is observed. All three complexes Mo1-Mo3 are subject to this regularity (Fig. 16) and therefore can be used interchangeably for chiroptical study of diamines.

V. Computational study

The results of ECD measurements allow to specify AC of examined ligands (1,2-aminols, *vic*-diamines, *etc.*), but are

purely qualitative since the structure of the adducts formed with auxiliary chromophores is unknown. Thus, with a view to answer the question about the nature of complexes formed *in situ* and the manner of complexation, we took the advantage of the higher extent solubility of dimolybdenum *tetrakis* (μ-pivalate) Mo2 and *tetrakis*(μ-isovalerate) Mo3 in solvents commonly used in spectroscopic studies compared to the currently used dimolybdenum tetraacetate Mo1. Numerous attempts to crystallize chiral dimolybdenum complex with all examined ligands were made. Furthermore, conditions developed in Z. Mayer[25] and C. A. M. Alfonso[26] groups for synthesis and separations of dirhodium carboxylates with α-amino acids were also applied to their molybdenum analogues. Despite our efforts to isolate the chiral adducts from reaction mixture, to synthesize dimolybdenum complex or obtain proper crystals for single crystal X-ray diffraction analysis, we were unable to succeed. For this reason we decided to apply calculations to provide an insight into the structure of the chiral complexes formed *in situ* in solution.

As a model for computational study, the stock dimolybdenum *tetrakis*(μ-pivalate) complex $[Mo_2\{(O_2C_2(CH_3)_4\}]$ (Mo2) was chosen because of its short side chain compared to the respective μ-isovalerate (Mo3) analogue. Formation of different structural chiral Mo2-complexes with coordinated selected ligands, *i.e.* α-amino acid, α-hydroxy acid, 1,2-amino alcohol and 1,2-diamine was considered. In the calculations D-α-alanine (2, Ala), L-mandelic acid (4, MA), *S*-1-amino-2-propanol (9, APol), (1*S*,2*S*)-diaminocyclohexane (11, DACH) and 3-phenyl-propane-1,2-diamine (13, PhPDA) were used as chiral ligands. The uniform code name for considered dimolybdenum *tetrakis* (μ-pivalate) complexes with chiral ligands was applied: it begins with the type of chiral ligand; next – the bridged or chelated (chel) geometry of complexation is indicated; then the number of coordinated ligands (from 1 to 4) is given; and finally, details of the arrangement of ligands (*cis*, *trans*, or *s* from *semi-dissociated*) and differences in projection of the hydrogen atoms (by a or b letters) are specified.

The structures were obtained by subsequent replacement of one or more pivalate group(s) in the stock complex by a chiral moiety(ies). The geometry optimizations and thermochemistry calculations were performed by using the hybrid Becke three-parameter Lee–Yang–Parr density functional theory (DFT) B3LYP functional[27,28] combined with LANL2DZ basis set and electron core potential[29,30] for the molybdenum atoms, and the 6-31+G(d) basis set for C, N, H, O atoms.

For the obtained structures, UV/ECD spectra were calculated with TD-DFT methods computing the first 50 electronic transitions. To this aim B3LYP, and the long range corrected version of B3LYP using the Coulomb-attenuating method CAM-B3LYP[31] functionals, combined with 6-311G(d,p) basis set for C, N, H, O atoms, and LanL2DZ with core potential for the Mo atom were applied. CAM-B3LYP provided results superior to those of B3LYP and only its results are shown in the manuscript. This is consistent with the conclusions of other papers in which different functionals were tested for calculating the ECD spectra.[32–35] The full UV/ECD TD-DFT/B3LYP data are collected in the ESI† section.
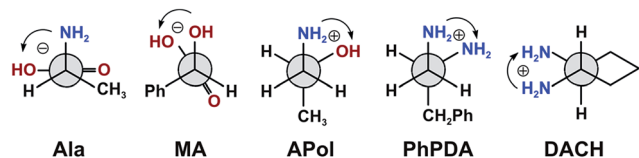
Fig. 17 Conformers of model chiral ligands considered in the calculations.

The ECD spectra were simulated by overlapping Gaussian functions for each transition utilizing the *SpecDis* ver. 1.61 program.[36] A Gaussian band-shape was applied with 0.35 eV as a half-height width. All the calculated UV/ECD spectra have been shifted by the value of difference of maximum absorption of the experimental and calculated UV spectra.[37]

Solvent effects were taken into account for both optimization and UV/ECD spectra calculations employing the integral equation formalism (IEF) version of the polarizable continuum model PCM[38,39] and using the dielectric constant for acetonitrile and chloroform equal to 35.688 and 4.7113, respectively. All the calculations were performed by using the Gaussian 09 package of programs.[40]

A plethora of possible conformers in each group of considered structures is expected due to: (1) arrangements of the chiral ligands bonding type (bridged, chelated, or axial); (2) rotation around the single C–C, N–C or C–N bonds; (3) way of complexation (*via* hydroxy or amino groups in case of **Ala** and **APol** ligands). Therefore, to restrict the number of conformers, some below assumptions were taken into account based either on our previous experience or on the literature data. Per analogy to our previous study on chiral Mo₂-complexes formed with *vic*-diols,[11] bridged and chelated (chel) structures were considered. Structures with axial arrangements of the chiral ligands were excluded from further consideration because of very long axial Mo⋯L distances, where L is a ligand. Therefore, the axial bonding to the $Mo_2(O_2CR)_4$ molecules is always weak. This is in contrast to the strong axial bonding to rhodium, chromium, ruthenium, *etc.*, in $Me_2(O_2CR)_4$ compounds (Me = transition metal).[23]

In the calculations of possible chiral Mo₂-complexes only gauche conformers with an antiperiplanar orientation of X–C–C–R unit(s) have been taken into account (X = N or O). This results from the fact that in this position the (Mo–X)–C–C–(X–Mo), where X is O or N, the torsional angle of about ±60° is well-suited for the ligation, and bulky R-groups point away from the rest of the complex and tend to avoid the steric interaction with the remaining carboxylate ligands in the stock complex (Fig. 17).

When choosing conformers for the calculation of α-amino and α-hydroxy acids we took the evidence in published literature relating two possible ways of complexation by this class of ligands into account. The first way involves the exchange of the pivalate group in the starting complex for the chiral ligand, through two oxygen atoms of carboxylate group of the amino acid.[23,41–43] Another possibility is complexation *via* two hydroxy groups when α-hydroxy acids are used, or through hydroxy and amino group in case of α-amino acids.[25,26] Such incorporation of a chiral ligand into the metal core causes the disturbance of chromophore D_{4h} symmetry.

Despite the adoption of these assumptions reducing the number of studied systems, the calculations are extremely time-consuming resulting in a total CPU time of *ca.* 350 000 hours. Moreover, in each class of compounds only few structures possessing the same number of atoms (and therefore the same number of basis sets) can be compared energetically. In the Table 1 ESI† the mono- and disubstituted bridged and chelating structure energies and population factors based on the ΔG values are gathered. However, the energetic comparisons must be treated with caution and reserve as values obtained at the DFT level are only approximate. Even for ground state flexible main-group compounds much better estimation of energetics can be achieved by including electron correlation effects in a more explicit way, as given in perturbational or post-Hartree–Fock methods.[44–46] The theoretical study of transition metal (TM) complexes excited states is significantly more challenging because of more complicated electronic structure of such compounds which involves the d shell of the metal surrounded by ligand with different acceptor/donor properties. Moreover, dimetallic TM systems often have an inherently multi-configurational character[47–49] and require theoretical method which deal with dynamic and non-dynamic correlation effects equally well and in principle, multi-configurational methods are preferred for such systems. However, application of such methods is still restricted to small or medium-size systems. Therefore, TD-DFT method is a compromise between accuracy and cost of the calculations.

Last but not least, small HOMO/LUMO energy gaps in the systems studied here probably caused a slow convergence of the optimization procedure, or problems with obtaining the ECD spectra. Thus, the SCF = Fermi converger is the necessary "keyword" to successfully end this type of calculations.

α-Amino acids

Based on the above, we decided to apply ligation only by COOH group in the bridged complexes (Fig. 18 and S8†).[23,41–43] This
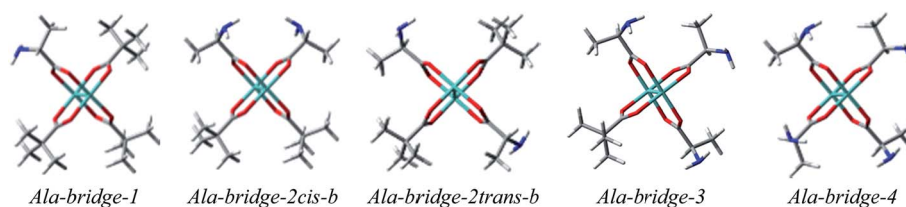

Ala-bridge-1   *Ala-bridge-2cis-b*   *Ala-bridge-2trans-b*   *Ala-bridge-3*   *Ala-bridge-4*

Fig. 18 Optimized selected structures of bridged D-α-alanine (**2**) Mo₂-complexes.
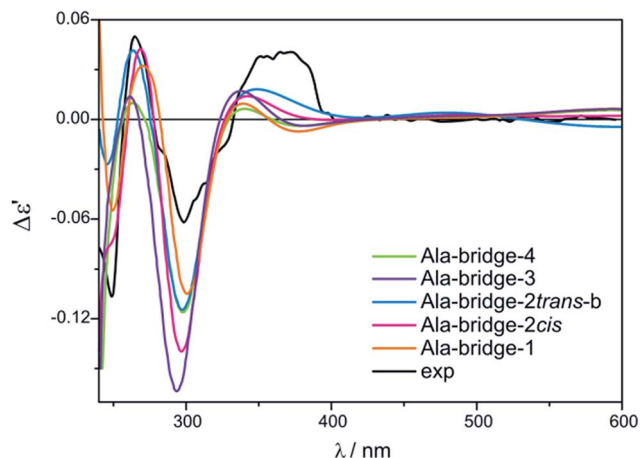
Fig. 19 Comparison of the CAM-B3LYP calculated ECD spectra of selected bridged **Ala**-complexes with experimental data.

choice seems reasonable due to the formation of hydrogen bond interaction between NH_2 and one of oxygen from carboxylic group which stabilize this kind of adducts.

Calculations indicate that the bridge structures are in good concordance with the experimental spectrum of D-α-alanine (**2**). Furthermore, the resulting UV-Vis and ECD spectra depend slightly on the number of exchanged carboxylic groups (Fig. 19). Therefore it is difficult to unambiguously judge which bridge complex dominates in the solution. This means that at this stage of research, we cannot precisely say how many pivalate groups have been replaced by carboxylate(s) of amino acids in the predominant complex formed *in situ*.

We have also performed the calculations of chelated Mo_2-amino acid complexes in which both NH_2 and COOH groups interact with one of the Mo atoms (Fig. S10†). The **Ala-chel-1c** monosubstituted complex is stabilized by intermolecular interactions (between the semidissociated pivalate groups and amine group of the chiral ligand). Furthermore, we considered also disubstituted chelated structures. The **Ala-chel-2b** was structurally analogical to the dirhodium complex presented independently by Frade[26] *et al.* and Majer *et al.*[25] The next complex, **Ala-chel-2**, is related to the previous one, yet binding to the transition metal *via* two oxygen atoms of the carboxylate unit. However, the behavior of the chelating structures of Mo_2-amino acid complexes mismatched the experimental data,
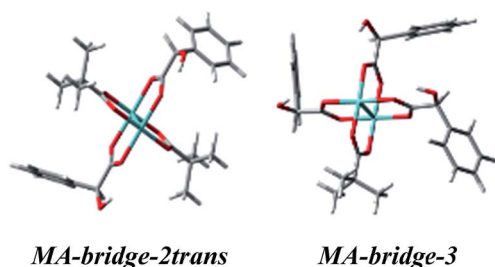
(Fig. S11 and S12†) suggesting that the Mo_2-core prefers bridge over chelating arrangement of amino acid ligands. In conclusion, we can say that the molybdenum complexes do not undergo the same mechanisms to exchange their achiral ligands as rhodium complexes.

α-Hydroxy acids

Treating the α-hydroxy acids as oxygen analogs of α-amino acids we can assume that they will be subject to the same ligation mode as α-amino acids. In the case of the bridged **Mo2-MA** complexes (Fig. S14†), broad ECD bands occur with the maximum nearby 600 nm. These bands come from a combined excitation of metal d–d orbitals and d-phenyl ring transitions of the chiral ligand. The calculated ECD spectra for all bridged D-α-mandelic acid (**4**) complexes (Fig. S15,† left) reflect the experimental negative and positive bands at around 600 and 380 nm, respectively. The third experimental band at 310 nm is not fully-resolved and appears as a local minimum. The calculated ECD spectra of only two structures: **MA-bridge-2trans** and **MA-bridge-3** (Fig. 20) match this band (Fig. 21).

In the diagnostic spectral range between 300–600 nm we observe mismatching behavior of CEs in the simulated spectra of the chelated complexes (Fig. S17†) with respect to experiment (Fig. S15,† right). Therefore, we can conclude that this way of ligation is not favored.

On the basis of the results received for α-hydroxy acids it may be summarized that the bridge structures reproduce the experimental data more precisely and can be considered dominant in the solution, which is consistent with our prediction.

1,2-Amino alcohols

We continue our calculations of dimolybdenum chiral adducts for amino alcohols according to the scheme specified in the general considerations. Complexes of *vic*-amino alcohols with dirhodium tetraacetate indicated coordination of the chiral ligand to the equatorial position.[50] However, formation of

MA-bridge-2trans   **MA-bridge-3**

Fig. 20 Optimized structures of selected bridged D-α-mandelic acid (**4**) Mo_2-complexes the best matching the experimental ECD spectra.
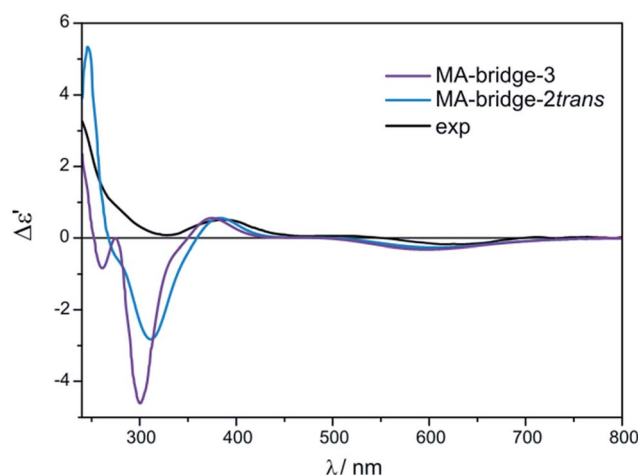

Fig. 21 Comparison of the CAM-B3LYP calculated ECD spectra of selected bridged **MA**-complexes with experimental data.
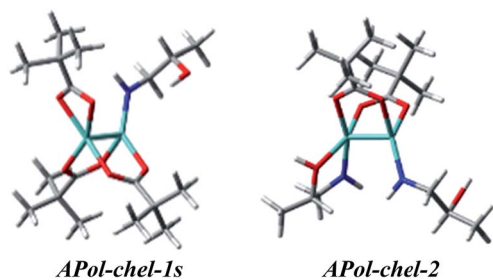
Fig. 22 Optimized structures of selected mono- and disubstituted chelated (chel) S-1-amino-2-propanol (**9**) Mo₂-complexes.
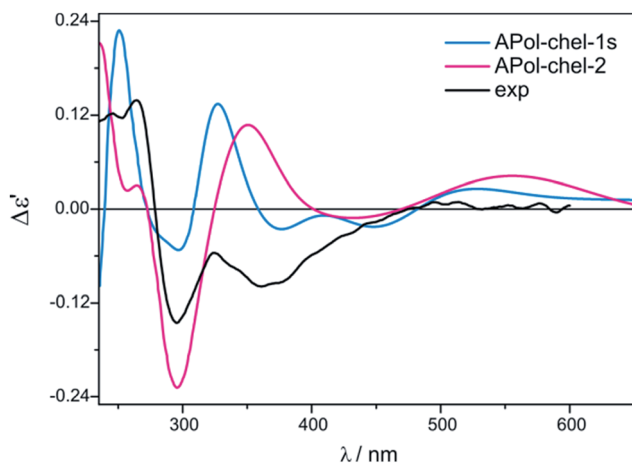

Fig. 23 Comparison of the CAM-B3LYP calculated ECD spectra of selected chelated **APol**-complexes with experimental data.

equatorial bridged or chelated structures was neither confirmed nor excluded. Initially we thoroughly examined the bridged complexes shown in Fig. S19.† The shape of the simulated curves, obtained for these structures, with one to three coordinated ligand(s), mismatches the experimental data (Fig. S20†).

Chelated structures of **APol** (**9**) obtained by the optimization procedure are shown in Fig. S23.† Among these structures, there are two with a semidissociated pivalate group. However, after comparing the simulated ECD spectra with the spectrum of *S*-(−)-1-amino-2-propanol (**9**) complexes with **Mo2** it can be stated that only **APol-chel-2** and **APol-chel-1s** structures (Fig. 22) well reproduced the diagnostic band at around 300 nm (Fig. 23) while it is mismatched by other semidissociated structures (Fig. S24†).
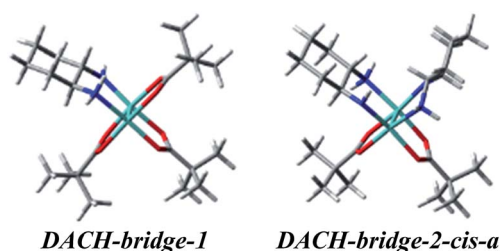

Fig. 24 Optimized structures of selected bridged (1S,2S)-diaminocyclohexane (**11**) Mo₂-complexes.

The CE at 320 nm, which in the experimental spectrum occurs as a local maximum, is reflected in spectra of **APol-chel-2** and **APol-chel-1s** chiral adducts as a well-developed positive ECD band. However, for the former complex this band is shifted *ca.* 30 nm towards the lower energy spectral range. The next experimental band, however, at 360 nm is only present in the latter complex spectrum. Deeper analysis of the shape of this experimental band suggests that its wideness might be caused by overlapping of another bands of lower intensity or may come from not fully-resolved CEs at 320 and 360 nm.

Such a spectral picture would correspond to the two small-intensity bands calculated for **APol-chel-1s**, or to broad ECD band of **APol-chel-2** shifted to *ca.* 430 nm. The spectra of other chelated structures exhibit no compliance with the experiment (Fig. S24,† right).

Thus, it seems that the chelated structure is predominant in the solution of *vic*-amino alcohols, but their type cannot be unequivocally determined from the calculations undertaken.

1,2-Diamines

Two different *vic*-diamines **DACH** (**11**) and **PhPDA** (**13**) were considered (Fig. 17) for the simulation of UV-Vis and ECD spectra. For the calculations we adopted both bridging and chelate structure of the adducts. For each of them UV-Vis and ECD spectra were calculated. Next, resulting ECD bands were compared with three CEs appearing in experimental spectra in the 280–410 nm range.

Among considered bridged **DACH** structures (Fig. S27†), the **DACH-bridge-1** and **DACH-dridge-2-*cis*-a** structures (Fig. 24) reproduced the best two experimental short-wavelength ECD bands (Fig. 25). However, the long-wavelength CE is not reflected by any of bridged **DACH** adducts (Fig. S28†). Moreover, the shift towards the lower energy field of all ECD bands in simulated spectra of bridged complexes can be seen with increasing number of coordinated chiral ligands to Mo₂-core.

On the other hand, the calculated ECD spectrum of chelated complex **DACH-chel-1b** (Fig. 26) nicely reproduces all CEs
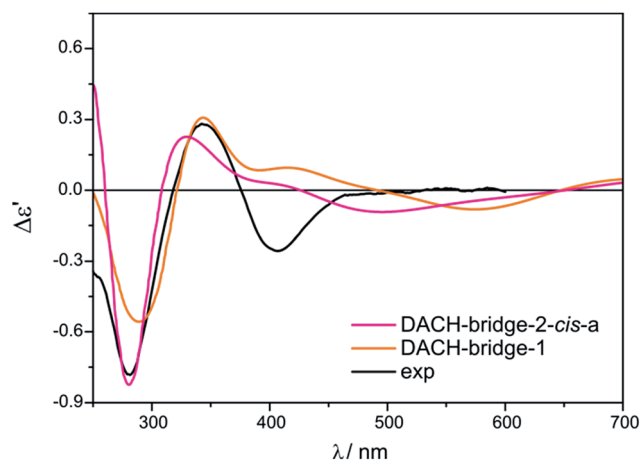

Fig. 25 Comparison of the CAM-B3LYP calculated ECD spectra of selected bridged **DACH**-complexes with experimental data.
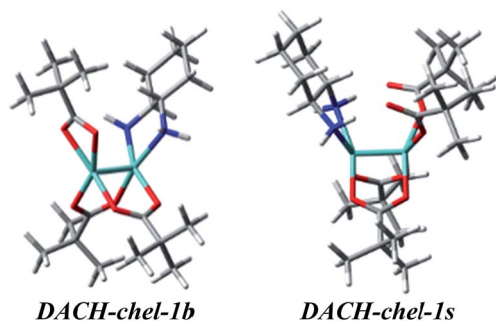
Fig. 26 Optimized structures of selected chelated (1S,2S)-diaminocyclohexane (11) Mo₂-complexes.
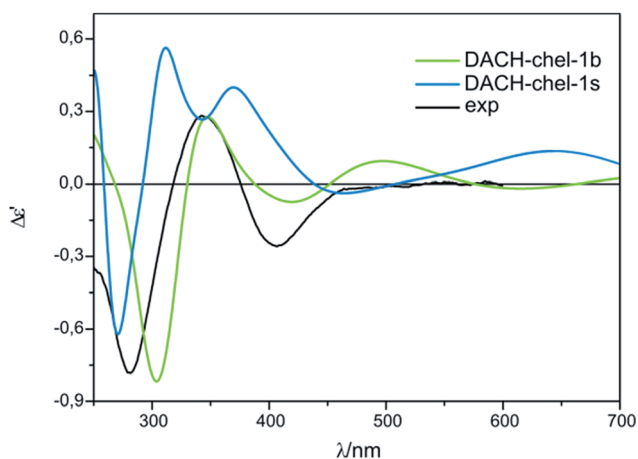

Fig. 27 Comparison of the CAM-B3LYP calculated ECD spectra of selected chelated **DACH**-complexes with experimental data.

(Fig. 27). Admittedly, the ECD band at around 300 nm is shifted by *ca.* 25 nm towards lower field compared to experiment, yet the remaining bands fit the measured ECD curve perfectly. In the **DACH-chel-1b** adduct there are some intermolecular NH⋯O interactions further stabilizing this structure.

The **DACH-chel-1s** complex in which the two semi-dissociated pivalate groups interact with the hydrogens from amino groups of chiral ligands was also taken into account. This type of complexation was postulated to be predominant in the solution of chiral 1,2-diol adducts with dimolybdenum tetrapivalate.[11] The ECD calculations for *vic*-diols were performed with the B3LYP functional, which in the case of **DACH**–Mo₂-complexes studied here, predicts a different shape of the ECD curves than CAM-B3LYP does (Fig. 28). In general, position and sign of only one ECD band (at *ca.* 290 nm) of chelated complexes is common for both functionals. Moreover, the CE around 400 nm at B3LYP and CAM-B3LYP levels are of opposite signs. Therefore, one must treat the computational ECD results with caution and reserve, and carefully outline the conclusions. So, taking into account the CAM-B3LYP results as more reliable in comparison to B3LYP,[32–35] it can be postulated that mono-substituted, chelated hydrogen bonded structures dominate in the solution of **DACH** with **Mo2**.

Because of computational problems with the optimization procedure for **DACH** complexes we decided to run an additional diamine chiral ligand, namely **PhPDA** (Fig. 17). Similarly to **DACH** complexes the formation of both bridged and chelated structures was considered and UV-Vis and ECD spectra were calculated at the same level of theory.

Again, for bridged structures (Fig. S32†) the calculated spectra did not exactly reflect the experimental data (Fig. S33†). As for the **DACH** complexes, only two experimental short-wavelength ECD bands are well reproduced by the **PhPDA-bridge-1** and **PhPDA-bridge-2-*cis*-a** structures. Calculated ECD spectra of the other bridge structures differ significantly from the experimental spectrum data (Fig. S33†).

On the other hand, among mono- and disubstituted chelating **PhPDA** complexes (Fig. S36†) the best fit to the measured ECD spectra was obtained for the **PhPDA-chel-1** complex as all CEs were predicted with a correct sign (Fig. 29). We also considered the structure with two semidissociated pivalate groups interacting by the hydrogen bonding with amine groups. However, despite the fact that the minimum was localised, its ECD calculations failed without specific cause.

Concluding the 1,2-diamines section: the simulated ECD spectra of chelated mono-coordinated dimolybdenum *tetrakis*(μ-pivalate) complexes are in good concordance with the
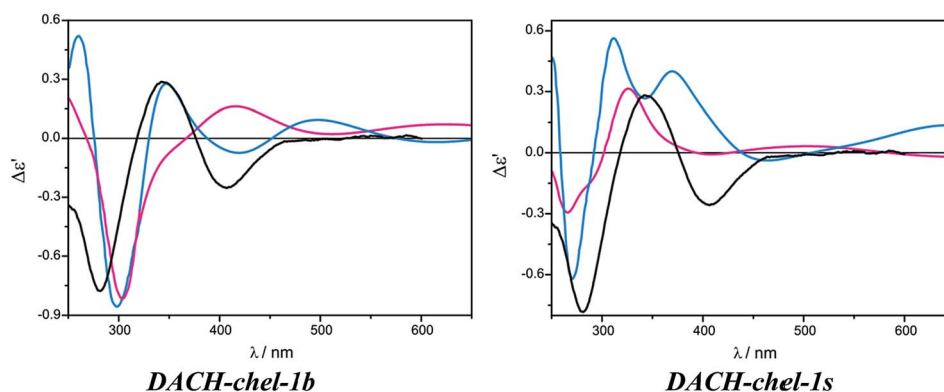

Fig. 28 Comparison of the CAM-B3LYP (blue line) and B3LYP (red line) calculated ECD spectra of chelated **DACH-chel-1b** (left) and **DACH-chel-1s** (right) complexes with experiment (black line).
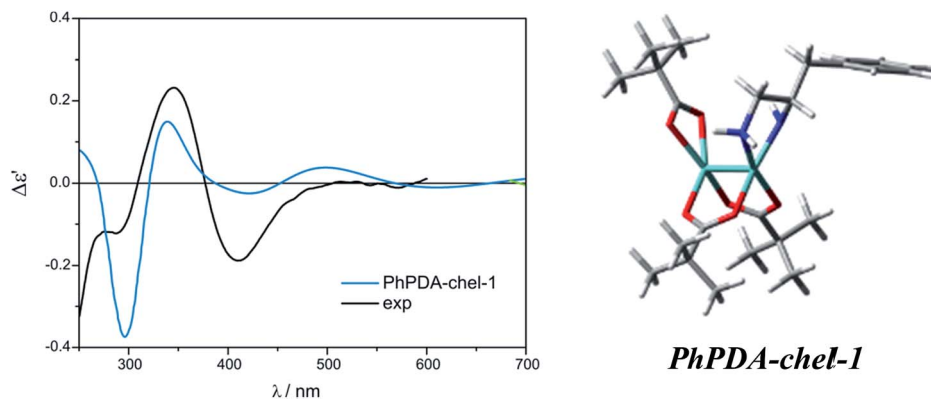
Fig. 29 Comparison of the CAM–B3LYP calculated ECD spectrum of chelated **PhPDA**-complex with **Mo2** (right) with experimental data (left).

experimental spectra, which indicates that this type of Mo$_2$-complexes with diamines most likely prevail in the solution.

3. Conclusions

The main finding of the present study is proving the effectiveness of dimolybdenum *tetrakis*(μ-pivalate) (**Mo2**) and *tetrakis*(μ-isovalerate) (**Mo3**) as auxiliary chromophores. They constitute an alternative to dimolybdenum *tetrakis*(μ-acetate) (**Mo1**) which was so far the only chromophore used in dichroic studies of transparent compounds. Their utility in that regard has been confirmed for α-amino and α-hydroxy acids, *vic*-amino alcohols, and *vic*-diamines ligands. ECD spectra of *in situ* formed chiral Mo$_2$-complexes with these ligands allow unambiguous assignment of the AC based on the rules correlating signs of respective CEs with the structure of the investigated ligand. It is worth noting that the correlating rules for **Mo2** and **Mo3** are the same as those previously formulated for **Mo1**. The results showed that for the α-amino and α-hydroxy acids a hexadecant rule works efficiently while for *vic*-amino alcohols and *vic*-diamines successfully operate a helicity rule. Ultimately, both tested carboxylates serve as auxiliary chromophores equivalent to **Mo1**.

Another essential result of this work is the identification of the probable structure of the dominant chiral complex existing in solution by a combined experimental and theoretical analysis of the ECD spectra. Based on the comparison of these ECD spectra it can be concluded that in the case of α-amino and α-hydroxy acids the bridging mode of ligation dominates in solution. However, in the case of *vic*-amino alcohols and *vic*-diamines the chelating mode of binding of ligands to the metal core prevails.

It can be expected that the disclosed in the context of this work effectiveness of the *in situ* dimolybdenum methodology will affect its broader utilization for determining the absolute configuration of transparent compounds. The simplicity of the methodology consisting of simple mixing a chiral ligand with an achiral auxiliary chromophore is, in fact, its greatest advantage. An additional benefit of the method lies in the possibility for determining the absolute configuration of even

flexible molecules on the basis of the ECD spectra alone. This is related to the fact that after bonding to the metal core the internal conformational mobility of such molecules becomes substantially restricted due to the steric requirements of the stock complex.

In our work, we presented new dimolybdenum complexes with greater solubility to act as auxiliary chromophores in the *in situ* methodologies. Since each method has its benefits and limitations, the expansion of available research methods seems to be essential. As a result of our study, one gains a greater pallet of methods, allowing several parallel techniques to be used.[1] This is especially beneficial in doubtful cases, as such an approach allows a high degree of confidence when assigning the absolute stereochemistry of the molecules.

4. Experimental section

The ECD spectra were acquired at room temperature in CHCl$_3$, CH$_3$CN and DMSO (for UV-Spectroscopy, Fluka) on a Jasco J-715 and J-815 spectropolarimeters and were collected at 0.5 nm per step with an integration time of 0.25 s over the range 200–900 nm with 200 nm min^{-1} scan speed, 5 scans. For the ECD standard measurements the chiral ligands (*ca.* 0.003 M) was mixed with stock complex [Mo$_2$(O$_2$R$_3$)$_4$] (*ca.* 0.002 M) and dissolved in respective solvent (5 mL) so that the molar ratio of the stock complex to ligand was about 1 : 1.5, in general. Using the *in situ* dimolybdenum method one does not obtain quantitative values since the real complex structure as well as the concentration of the chiral complex formed in solution is not known. Therefore, the ECD data are presented as the Δε′ values. These Δε′ values are calculated in the usual way as $\Delta\varepsilon' = \Delta A/c \times d$, where c is the molar concentration of the chiral ligand, assuming 100% complexation (A = absorption; d = path length of the cell).

UV-Vis spectra were measured on a Varian spectrophotometer UV-Vis Carry 100E or on a Jasco V-670 UV-Vis-NIR spectrophotometer in CHCl$_3$, CH$_3$CN and DMSO.

Chiral ligands **1–15** were purchased from Fluka, Sigma-Aldrich, POCH or Alfa-Aesar and were used without further purification.

Acknowledgements

Literature

1 P. L. Polavarapu, *Chirality*, 2008, **20**, 664–672.

2 H.-G. Jeon, M. J. Kim and K.-S. Jeong, *Org. Biomol. Chem.*, 2014, **12**, 5464–5468.

3 N. Harada and N. Berova, in *Comprehensive Chirality*, ed. E. M. Carreira and H. Yamamoto, Elsevier, Amsterdam, 2012, pp. 449–477.

4 K. M. Specht, J. Nam, D. M. Ho, N. Berova, R. K. Kondru, D. N. Beratan, P. Wipf, R. A. Pascal and D. Kahne, *J. Am. Chem. Soc.*, 2001, **123**, 8961–8966.

5 H.-G. Kuball, E. Dorr, T. Höfer and O. Türk, *Monatsh. Chem.*, 2005, **136**, 289–324.

6 S. Superchi, D. Casarini, A. Laurita, A. Bavoso and C. Rosini, *Angew. Chem., Int. Ed.*, 2001, **40**, 451–454.

7 M. Górecki, E. Jabłońska, A. Kruszewska, A. Suszczyńska, Z. Urbańczyk-Lipkowska, M. Gerards, J. W. Morzycki, W. J. Szczepek and J. Frelek, *J. Org. Chem.*, 2007, **72**, 2906–2916.

8 Z. Pakulski, N. Gajda, M. Jawiczuk, J. Frelek, P. Cmoch and S. Jarosz, *Beilstein J. Org. Chem.*, 2014, **10**, 1246–1254.

9 M. Górecki, A. Kamińska, P. Ruśkowska, A. Suszczyńska and J. Frelek, *Pol. J. Chem.*, 2006, **80**, 523–534.

10 J. Frelek, M. Górecki, A. Suszczyńska, E. Forro and Z. Majer, *Mini-Rev. Org. Chem.*, 2006, **3**, 281–290.

11 M. Jawiczuk, M. Górecki, A. Suszczyńska, M. Karchier, J. Jaźwiński and J. Frelek, *Inorg. Chem.*, 2013, **52**, 8250–8263.

12 J. Frelek, N. Ikekawa, S. Takatsuto and G. Snatzke, *Chirality*, 1997, **9**, 578–582.

13 J. Frelek, G. Snatzke and W. J. Szczepek, *J. Anal. Chem.*, 1993, **345**, 683–687.

14 J. Frelek, P. Ruśkowska, A. Suszczyńska, K. Szewczyk, A. Osuch, S. Jarosz and J. Jagodziński, *Tetrahedron: Asymmetry*, 2008, **19**, 1709–1713.

15 J. Frelek, Z. Majer, A. Perkowska, G. Snatzke, I. Vlahov and U. Wagner, *Pure Appl. Chem.*, 1985, **57**, 441–451.

16 A. Murugan, V. K. Kadambar, S. Bachu, M. Rajashekher Reddy, V. Torlikonda, S. G. Manjunatha, S. Ramasubramanian, S. Nambiar, G. P. Howell and J. Withnall, *Tetrahedron Lett.*, 2012, **53**, 5739–5741.

17 K. Steele, P. Shirodaria, M. O'Hare, J. D. Merrett, W. G. Irwin, D. I. H. Simpson and H. Pfister, *Br. J. Dermatol.*, 1988, **118**, 537–544.

18 H. U. Blaser, *Chem. Rev.*, 1992, **92**, 935–952.

19 D. Saint-Léger, J.-L. Lévêque and M. Verschoore, *J. Cosmet. Dermatol.*, 2007, **6**, 59–65.

20 S. M. Thombre and B. D. Sarwade, *J. Macromol. Sci., Part A: Pure Appl. Chem.*, 2005, **42**, 1299–1315.

21 S. L. Bourke and J. Kohn, *Adv. Drug Delivery Rev.*, 2003, **55**, 447–466.

22 O. E. Owen, A. P. Morgan, H. G. Kemp, J. M. Sullivan, M. G. Herrera and G. F. Cahill Jr, *J. Clin. Invest.*, 1967, **46**, 1589–1595.

23 *Multiple bond between metal atoms*, ed. F. A. Cotton, C. A. Murillo and R. A. Walton, Springer Science and Business Media, Inc, 2005.

24 J. Frelek, A. Klimek and P. Ruśkowska, *Curr. Org. Chem.*, 2003, **7**, 1081–1104.

25 Z. Majer, G. Szilvágyi, L. Benedek, A. Csámpai, M. Hollósi and E. Vass, *Eur. J. Inorg. Chem.*, 2013, **17**, 3020–3027.

26 R. F. M. Frade, N. R. Candeias, C. M. M. Duarte, V. André, M. Teresa Duarte, P. M. P. Gois and C. A. M. Afonso, *Bioorg. Med. Chem. Lett.*, 2010, **20**, 3413–3415.

27 A. D. Becke, *J. Chem. Phys.*, 1993, **98**, 5648–5652.

28 *Electronic Density Functional Theory: Recent Progress and New Directions*, ed. K. Burke, J. P. Perdew and Y. Wang, Plenum, New York, 1998.

29 P. J. Hay and W. R. Wadt, *J. Chem. Phys.*, 1985, **82**, 270–283.

30 P. J. Hay and W. R. Wadt, *J. Chem. Phys.*, 1985, **82**, 299–310.

31 T. Yanai, D. P. Tew and N. C. Handy, *Chem. Phys. Lett.*, 2004, **393**, 51–57.

32 O. Julínek, V. Setnička, N. Miklášová, M. Putala, K. Ruud and M. Urbanová, *J. Phys. Chem. A*, 2009, **113**, 10717–10725.

33 W. Skomorowski, M. Pecul, P. Sałek and T. Helgaker, *J. Chem. Phys.*, 2007, **127**, 085102/085101–085102/085108.

34 X. Li, K. H. Hopmann, J. Hudecová, J. Isaksson, J. Novotná, W. Stensen, V. Andrushchenko, M. Urbanová, J.-S. Svendsen, P. Bouř and K. Ruud, *J. Phys. Chem. A*, 2013, **117**, 1721–1736.

35 R. Kobayashi and R. D. Amos, *Chem. Phys. Lett.*, 2006, **420**, 106–109.

36 T. Bruhn, A. Schaumlöffel, Y. Hemberger and G. Bringmann, *SpecDis version 1.62*, University of Würzburg, Würzburg, Germany, 2014.

37 G. Bringmann, T. A. M. Gulder, M. Reichert and T. Gulder, *Chirality*, 2008, **20**, 628–642.

38 B. Mennucci, *Wiley Interdiscip. Rev.: Comput. Mol. Sci.*, 2012, **2**, 386–404.

39 G. Scalmani and M. J. Frisch, *J. Chem. Phys.*, 2010, **132**, 114110/114111–114110/114115.

40 M. J. Frisch, G. W. Trucks, H. B. Schlegel, G. E. Scuseria, M. A. Robb, J. R. Cheeseman, G. Scalmani, V. Barone, B. Mennucci, G. A. Petersson, H. Nakatsuji, M. Caricato, X. Li, H. P. Hratchian, A. F. Izmaylov, J. Bloino, G. Zheng, J. L. Sonnenberg, M. Hada, M. Ehara, K. Toyota, R. Fukuda, J. Hasegawa, M. Ishida, T. Nakajima, Y. Honda, O. Kitao, H. Nakai, T. Vreven, J. A. Montgomery Jr, J. E. Peralta, F. Ogliaro, M. Bearpark, J. J. Heyd, E. Brothers, K. N. Kudin, V. N. Staroverov, R. Kobayashi, J. Normand, K. Raghavachari, A. Rendell, J. C. Burant, S. S. Iyengar, J. Tomasi, M. Cossi, N. Rega, N. J. Millam, M. Klene, J. E. Knox, J. B. Cross,

V. Bakken, C. Adamo, J. Jaramillo, R. Gomperts, R. E. Stratmann, O. Yazyev, A. J. Austin, R. Cammi, C. Pomelli, J. W. Ochterski, R. L. Martin, K. Morokuma, V. G. Zakrzewski, G. A. Voth, P. Salvador, J. J. Dannenberg, S. Dapprich, A. D. Daniels, Ö. Farkas, J. B. Foresman, J. V. Ortiz, J. Cioslowski and D. J. Fox, *Gaussian 09,* Revision D.01, Gaussian, Inc., Wallingford CT, 2009.

41 F. Apfelbaum-Tibika and A. Bino, *Inorg. Chem.*, 1984, **23**, 2902–2905.

42 A. Bino and F. A. Cotton, *J. Am. Chem. Soc.*, 1980, **102**, 3014–3017.

43 F. Apfelbaum and A. Bino, *Inorg. Chim. Acta*, 1989, **155**, 191–195.

44 J. C. Dobrowolski, M. H. Jamróz, R. Kołos, J. E. Rode and J. Sadlej, *ChemPhysChem*, 2007, **8**, 1085–1094.

45 J. C. Dobrowolski, M. H. Jamroz, R. Kolos, J. E. Rode, M. K. Cyranski and J. Sadlej, *Phys. Chem. Chem. Phys.*, 2010, **12**, 10818–10830.

46 B. Boeckx, W. Nelissen and G. Maes, *J. Phys. Chem. A*, 2012, **116**, 3247–3258.

47 M. Brynda, L. Gagliardi and B. O. Roos, *Chem. Phys. Lett.*, 2009, **471**, 1–10.

48 S. J. Tereniak, R. K. Carlson, L. J. Clouston, V. G. Young, E. Bill, R. Maurice, Y.-S. Chen, H. J. Kim, L. Gagliardi and C. C. Lu, *J. Am. Chem. Soc.*, 2013, **136**, 1842–1855.

49 D. Escudero and W. Thiel, *J. Chem. Phys.*, 2014, **140**, 194105/194101–194105/194108.

50 J. Frelek, M. Górecki, J. Jaźwiński, M. Masnyk, P. Ruśkowska and R. Szmigielski, *Tetrahedron: Asymmetry*, 2005, **16**, 3188–3197.